

# Structure-Related Electrochemistry of Sulfur-Poly(acrylonitrile) Composite Cathode Materials for Rechargeable Lithium Batteries

Jean Fanous,<sup>†</sup> Marcus Wegner,<sup>†</sup> Jens Grimminger,<sup>†</sup> Anne Andresen,<sup>†</sup> and Michael R. Buchmeiser<sup>\*,‡</sup>

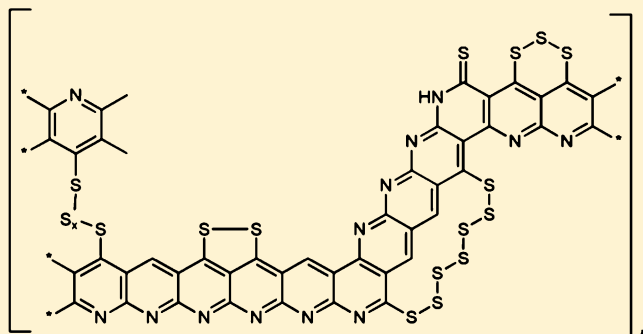
<sup>†</sup>Robert Bosch GmbH, Corporate Sector Research and Advance Engineering (CR/ARC1), Postfach 10 60 50, 70049 Stuttgart, Germany

<sup>‡</sup>Institute of Polymer Chemistry University of Stuttgart, 70569 Stuttgart, Germany

## Supporting Information

**ABSTRACT:** The structure of sulfur-poly(acrylonitrile)-based Li-sulfur batteries is elucidated and correlated with the electrochemical performance of such devices. Apart from the poly(acrylonitrile)-derived backbone, thioamide as well as poly(sulfide) structures are proposed. Furthermore, the intermediary formation of  $S_8$  during cycling and the role of the electrolyte in its reintegration during charging into are addressed. In summary, a comprehensive picture of the chemistry and electrochemistry of Li-sulfur batteries is presented.

**KEYWORDS:** cathode materials, polymer-sulfur composite, rechargeable lithium battery, conducting polymer, poly(acrylonitrile)



## INTRODUCTION

In view of limited resources for raw materials and energy, energy-storage systems have moved into the center of interest, batteries certainly being the most prominent ones. The viability of any battery-based concept strongly depends on a few issues which are apart from the prize (i) safety of the device, (ii) high energy density, and (iii) good cycling stability. Among the most promising element combinations for the next generation of batteries is lithium/sulfur. The theoretical specific capacity of elemental sulfur for  $S + 2e^- \rightarrow S^{2-}$  is 1672 mA h/g, which is the highest of any solid cathode material. Together with lithium ( $2 Li \rightarrow 2 Li^+ + 2e^-$ ), the theoretical specific energy density amounts to 2600 W h/kg. However, in view of the status quo in high energy density battery applications, the energy density of lithium battery systems has to be improved essentially. To do so, we need to fully understand its chemistry and physics.

Because of the insulating nature of sulfur, the cathode of Li/S batteries must contain an additional conducting additive, e.g., carbon black, in combination with a binder and a nonaqueous electrolyte, e.g., carbonates or ethers, to ensure for a complete contacting of the sulfur. Starting from elemental sulfur, i.e., from  $S_8$ , the electrochemical reduction cascade finally leads to poly(sulfide)s,  $S_x^{2-}$ , which are soluble in the chosen electrolyte for at least  $x \leq 3$ . Consequently, diffusion of active cathode material, i.e. of poly(sulfide)s to the anode occurs, resulting in the formation of  $Li_2S$  at the lithium surface and a sometimes dramatic loss in capacity. Several concepts for poly(sulfide) retention have been investigated. Nazar et al. presented a highly ordered nanostructured, mesoporous, and modified carbon sulfur cathode, which helps to retard the diffusion of

poly(sulfide)s from the cathode, thereby minimizing the loss of active mass in the cathode and improving cycling stability.<sup>1</sup> Scrosati et al. demonstrated that the use of a polymeric electrolyte can also lead to a prolonged retention of poly(sulfide)s within the cathode. Furthermore, organosulfides in which sulfur is covalently bound to a polymeric backbone were used.<sup>2</sup> Generally, these compounds show a reversible cleavage and formation of disulfide bridges. Major drawbacks of these materials are their very low specific capacities and poor cycling stabilities.<sup>3–6</sup> Very recently, porous hollow carbon-sulfur composites with excellent cycling properties have been reported.<sup>7</sup> An appealing system has been described by Wang et al.<sup>8</sup> Taking advantage of the well-known, though still poorly understood cyclization chemistry of poly(acrylonitrile) (PAN),<sup>9</sup> it was mixed with an excess of elemental sulfur and heated to 300 °C or higher. In course of this procedure, the sulfur dehydrogenates PAN, which forms cyclic structures with a conjugated  $\pi$ -system. Concomitantly,  $H_2S$  is released. This composite was then used as active cathode material showing a high specific capacity (800 mA h/g<sub>composite</sub>), good efficiency, low self-discharge, excellent cycling stability (380 cycles with 90% of the capacity after 5 cycles,  $Q_5$ ), and improved rate performance.<sup>10–14</sup> Nevertheless, despite these most favorable properties, until now the main question how the sulfur is embedded into the cyclic PAN-derived network, from now on referred to as cPAN, has not been answered satisfactorily. The

**Received:** August 19, 2011

**Revised:** October 11, 2011

**Published:** October 20, 2011

same accounts for the entire cycling chemistry. Wang et al. proposed that sulfur existed in its elemental state.<sup>10</sup> However, experiments carried out by Yu et al. indicated the existence of sulfur–carbon bonds.<sup>12</sup>

In view of the promising properties of PAN/sulfur (SPAN) composites as active cathode materials, it is inevitable to significantly extend the knowledge on the structure and fading mechanisms in order to be able to improve this system for a next generation of lithium batteries. Focusing on PAN/sulfur-based lithium ion battery systems, we were particularly interested in elucidating the structural features of such systems in order to correlate them with their cell performance. Here we report our results.

## ■ EXPERIMENTAL SECTION

**Synthesis of SPAN and ScPAN Composites.** SPAN was synthesized as reported<sup>8</sup> at 330 °C. ScPAN was prepared by heating PAN for 1 h to 250 °C under air to obtain cPAN (C:H:N:O 64.7:3.2:23.2:9.1). The black powder was then mixed with sulfur (25:75, wt %) and heated to 330 °C under nitrogen for 6 h. Finally, the composite was Soxhlet extracted with toluene for 6 h to remove any remaining sulfur (C:H:N:O 53.0:1.7:18.2:17.6:9.3).

**Cell Preparation.** The active material was mixed with carbon black (Super PLi, Timcal, Duesseldorf, Germany) and poly(vinylidene fluoride) (PVDF, Solef 6020, Solvay, Hannover, Germany) in a ratio of 70:15:15 (wt %) in N-methyl-2-pyrrolidone (1:10 w (active material)/w (solvent), VWR International). The dispersion was coated on aluminum foil (Roth, Karlsruhe, Germany) with a wet thickness of 400  $\mu\text{m}$  and then dried in vacuo. Test cells were prepared from Li metal foil as anode, celpard 2400 as separator, and a 1 M LiPF<sub>6</sub> solution in a mixture of ethylene carbonate (EC), dimethyl carbonate (DMC) and diethyl carbonate (DEC) (50:25:25, wt %, Ferro, Cleveland, U.S.) as electrolyte.

**Cycled Cathode Preparation (Sulfur Balance).** Five cells were prepared as described above, then either discharged once or discharged and then recharged, opened, washed twice with 20 mL of water, dried in vacuo, and then subjected to elemental analysis. Charged cells were first extracted with toluene to remove all elemental sulfur.

**Analytical Measurements.** TOF-SIMS spectra were collected on a TOF-SIMS 5 from ION-TOF (Münster, Germany). XPS analyses were performed on a PHI Quantera SXM spectrometer (Kanagawa, Japan) using a focused, monochromatized AlK $\alpha$  radiation (1486.6 eV) operated at a constant pass energy of 55 eV. The spectrometer was calibrated using the photoemission lines of Au (Au4f<sub>7/2</sub> = 83.96  $\pm$  0.1 eV), Ag (Ag3d<sub>5/2</sub> = 368.21  $\pm$  0.1 eV) and Cu (Cu2p<sub>3/2</sub> = 932.62  $\pm$  0.1 eV). For the Ag3d<sub>5/2</sub> line, the full width at half-maximum (fwhm) was 0.63 eV under recording conditions. The analyzed area had a diameter of 100  $\mu\text{m}$  and the pressure in the analysis chamber was in the 1  $\times$  10<sup>-9</sup> Torr range. FT-IR spectra were recorded on a Bruker Equinox-55 (Ettlingen, Germany), the RAMAN-spectra were recorded on a LabRAM ARAMIS Vis (HORIBA Jobin Yvon, Bensheim, Germany). Test cells were tested with the BaSyTec – battery test software (Asseltingen, Germany).

## ■ RESULTS AND DISCUSSION

The synthesis of SPAN was carried out following the procedure reported by Wang et al.,<sup>10</sup> which entails the reaction of PAN with S<sub>8</sub> at 330 °C in the absence of O<sub>2</sub>. Elemental analysis revealed a sulfur content of 41  $\pm$  1 wt %, which formally corresponds to one sulfur atom per repeat unit, i.e., per acrylonitrile-derived C<sub>3</sub>N-unit (vide infra, Figure 3). During this reaction, elemental sulfur is incorporated into the network while supporting the dehydrogenation of PAN, resulting in the formation of H<sub>2</sub>S. In order to separate the cyclization of PAN from the incorporation of sulfur, a two-step synthesis was carried out. First, the dehydrogenation of PAN under oxygen,

resulting in cyclized PAN (cPAN) was performed as described in the literature.<sup>13,15</sup> Then, S<sub>8</sub> was added and the mixture was heated to 300 °C. We wish to refer to the material prepared this way as ScPAN. The C/N weight-ratio of all composites, i.e. of SPAN and ScPAN as measured by elemental analysis was in the range of 2.8–3.0, which is somewhat higher than the theoretical value for a perfect 6-membered ring-based, polyannelated pyridine system (C/N = 2.6, Figure 3). We attribute this slightly elevated C-content to some sulfur-free 2D graphite-type fragments inside the polymeric network that are formed in course of the cyclization of PAN.<sup>9</sup> And in fact, the Raman spectra show the typical signals of a graphitic structure around range of 1330–1560 cm<sup>-1</sup> (see Figure S1 in the Supporting Information).

To identify the content of elemental sulfur, both composites, i.e., SPAN and ScPAN were extensively washed with toluene in a Soxhlet extractor. This procedure ensured for a complete removal of any S<sub>8</sub>. In case the SPAN reaction was stopped before all excess of sulfur had evaporated, a higher sulfur content, i.e., 48 wt %, was detected. However, after extraction with toluene, the S-content as determined by elemental analysis was the same within experimental error for all composites, i.e., 41  $\pm$  1 wt %. This strongly suggests that the entire sulfur found in thoroughly washed SPAN or ScPAN is covalently bound to the polymer backbone. This is further supported by the fact that after Soxhlet extraction, X-ray diffraction (XRD) measurements do not show any signals for elemental sulfur (see Figure S2 in the Supporting Information). Further proof is provided by the voltage profiles. Compared to the discharge curves of a composite containing 42 wt % of sulfur, which starts to discharge at  $U = 1.8$  V, the one of a composite having 48 wt % of sulfur, i.e., ca. 6 wt % of S<sub>8</sub>, starts to discharge at a higher voltage around  $U = 2.4$  V, which is in fact a direct result of residual free S<sub>8</sub> (see Figure S3 in the Supporting Information). After its reduction, the voltage is reduced to approximately 1.7 V and becomes comparable to the one of a composite containing ca. 42 wt % sulfur. Thus, a first important finding is that PAN-sulfur composites prepared at  $T = 330$  °C can bind sulfur up to 42 wt % in a fully covalent manner. Notably, the findings reported by both Wang and Yu on free sulfur in such composites were obtained with composites prepared from large amounts of sulfur. Apparently, not all excess sulfur had evaporated there.

Next, we tried to elucidate how the sulfur is bound to the composite. Generally, there are at least three possibilities for sulfur to be embedded in a PAN matrix. As suggested by Wang<sup>10</sup> and Yu<sup>12</sup> sulfur can be nanodispersed in an elemental state or be covalently bound to carbon. In addition, sulfur covalently bound to nitrogen can be imagined, however, such structures appear less probable since the conjugated  $\pi$ -system of cPAN would be significantly disturbed. Finally, thioketone fragments must be taken into account. Because the results described above clearly rule out the presence of any nanodispersed S<sub>8</sub>, the type of binding of sulfur to carbon (and eventually to nitrogen) had to be elucidated. In view of the results reported by Yu et al.,<sup>12</sup> who suggested the existence of C–S bonds, we recorded TOF-SIMS-spectra of both the SPAN and ScPAN composite (Figure 1a). Different CNS-fragments, e.g., CNS<sup>-</sup> and C<sub>3</sub>NS<sup>-</sup> at  $m/z = 58$  and  $m/z = 82$ , respectively, were observed. Additionally, CS fragments (C<sub>2</sub>S<sup>-</sup>,  $m/z = 56$ ) were detected, however, no SN fragments ( $m/z = 46$ ). This supports the assumption that sulfur is exclusively bound to carbon but not to nitrogen. Nevertheless,

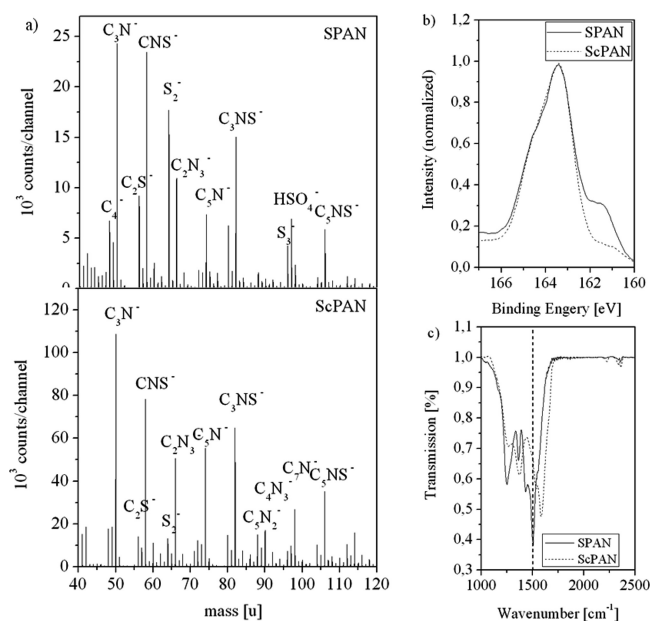


**Figure 1.** SPAN and ScPAN. (a) TOF-SIMS spectra, (b) XPS spectra ( $S_{2p}$ ), and (c) FT-IR spectrum, showing the thioamide signal at  $1500\text{ cm}^{-1}$  (dash marked).

the very intense signal at  $m/z = 58$  ( $CNS^-$ ) suggests that a significant amount of sulfur is bound to carbon atoms next to nitrogen. Finally, signals for  $S_3^-$  ( $m/z = 96$ ) were recorded, indicative for oligosulfide structures. Further information on the structure was received by XPS spectroscopy. The  $S_{2p}$ -spectra of SPAN and ScPAN displayed different shapes (Figure 1b). The signal at  $163.5\text{ eV}$  represents the sulfur's  $2p$  electron, either bound to carbon or to sulfur as in organodisulfides.<sup>16</sup> Due to the very similar binding energies, those states cannot fully be distinguished by means of XPS.<sup>17,18</sup> However, in contrast to ScPAN, a pronounced shoulder at  $161.5\text{ eV}$  is observed in SPAN. There, the shift to lower binding energy suggests a sulfide-type state of sulfur.<sup>19–21</sup> The FT-IR spectra showed different signals for both SPAN and ScPAN. Sulfides usually give rise to absorptions in the range of  $2400\text{ cm}^{-1}$  and  $1800\text{ cm}^{-1}$  (Figure 1c). In this range, the signals for SPAN and ScPAN are quite similar. However, an intense signal at  $1500\text{ cm}^{-1}$  was observed only in SPAN. This signal can be assigned to thioamide structures, in which the sulfur has the same oxidation state as in sulfides.<sup>22</sup>

This very particular difference between SPAN and ScPAN clearly correlates with the way in which these composites have been prepared. Thus,  $H_2S$  is produced in course of the synthesis of SPAN, which can react with the nitrile groups of PAN, resulting in the formation of thioamides according to  $R-CN + H_2S \rightarrow R-(C=S)-NH_2$ . In contrast, ScPAN formed in a two-step synthesis cannot contain any significant amounts of thioamides, since probable most nitrile groups have undergone thermally induced cyclization to form pyridine units before any sulfur is added. Consequently, a significant fraction of the  $CNS^-$  fragments in the TOF-SIMS of SPAN must stem from the thioamide groups in SPAN, however, a different functional group also fragmenting into  $CNS^-$  must exist in ScPAN because of the intense  $CNS^-$  signal in its TOF-SIMS spectrum. One plausible explanation is the presence of 2-pyridylthiolates and/or 2- $S_x^-$ -pyridyl structures (Figure 3) formed via  $S_8$ -induced dehydrogenation of cPAN. In conclusion, our measurements strongly suggest that the entire sulfur in SPAN is bound to carbon and exists in the form of oligo(sulfide)s, 2-pyridylthiolates, as well as in the form of thioamide structures.

The next question of utmost importance was about the electrochemistry of SPAN and the fate of the oligo(sulfide)s during cycling. Both Wang et al. and Yu et al. cycled their cells with  $LiPF_6$  in a mixture of carbonates, i.e., ethylencarbonate (EC), propylencarbonate (PC), dimethylcarbonate (DMC) and diethylcarbonate (DEC).<sup>10,12</sup> However, conventional Li-sulfur cells, containing only sulfur, carbon, and binder in the cathode, are prepared from lithium bis(trifluoromethylsulfon)imide ( $LiTFSI$ ) in a mixture of 1,3-dioxolane (DOL) and dimethoxyethane (DME).<sup>23</sup> Therefore, the influence of both the Li-ion conducting salt and different solvents on the cell performance was studied. Figure 2 reveals that the two different Li-ion-conducting salts used, i.e.  $LiPF_6$  and  $LiTFSI$ , do not have any significant influence on cell performance, instead, the solvent turned out to be the relevant parameter. In fact, the crucial difference of the solvent systems investigated is the solubility of poly(sulfide)s therein. In contrast to a mixture of carbonates, mixtures of DOL and DME are perfect solvents for these intermediates. In Figure 2b, the discharge profile of a cell prepared from  $LiTFSI$  in DOL:DME shows a shoulder, which can be correlated with the formation of elemental sulfur according to Figure S3 in the Supporting Information. During reduction, the sulfur of the poly(sulfide)s that is not bound to carbon but to sulfur is first released from the backbone according to  $R-S-S_x^- + 2 e^- \rightarrow R-S-S_y^- + (x-y)S^{2-}/S_{x-y}^{2-}$ .

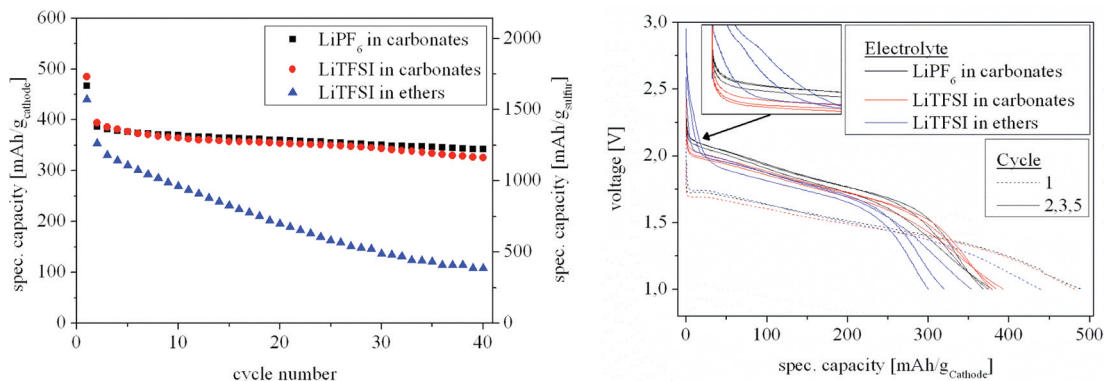


**Figure 2.** (a) Capacity and (b) voltage profile of SPAN cells, cycled with different electrolytes. C-rate was  $C/10$ . Theoretical capacity of the SPAN shown here was  $468\text{ mA h/g}_{\text{cathode}}$ .

$\text{Li}_2\text{S}_{x-y}$  is then further reduced to  $\text{Li}_2\text{S}$  ( $2x-2 \text{ Li} + \text{Li}_2\text{S}_{x-y} \rightarrow x-y \text{ Li}_2\text{S}$ ) and finally reoxidized to elemental sulfur during recharging. As a consequence, a continuous diffusion of poly(sulfide)s, permanently formed during cycling to the anode occurs – as is known for lithium–sulfur cells.

It was therefore important to find out how much sulfur was directly bound to carbon and to calculate the amount of poly(sulfide)s that are released during discharge. We therefore established a sulfur balance with  $\text{LiPF}_6$  in EC/DMC/DEC as well as with  $\text{LiTFSI}$  in DME/DOL, measuring the sulfur content of a 42 wt % composite in the discharged and charged state, respectively. For the charged state, the sulfur content was separated into covalently bound, sulfidic ( $\text{S}_x^{2-}$ ) and elemental sulfur by using a toluene Soxhlet extraction (Table 1). Both in

**Table 1. Mass Balance for Sulfur in Different States of Charge (SOC) of SPAN Cells<sup>a</sup>**

	discharged		charged		
	C–S <sup>-</sup>	S <sub>x</sub> <sup>2-</sup>	covalently bound S	S <sub>x</sub> <sup>2-</sup>	S <sub>8</sub> <sup>b</sup>
LiPF <sub>6</sub> in carbonates	30	70	51	5	44
LiTFSI in ethers	30	70	51	12	37

<sup>a</sup>Values represent the average of 5 devices. <sup>b</sup>Determined by Soxhlet extraction with toluene.

the charged and discharged state, the same amounts of covalently bound sulfur were found for both solvents. And in fact, the C–S<sup>-</sup>:S<sub>x</sub><sup>2-</sup> ratio of 3:7 suggests the presence of C–S<sub>x</sub>–S–C structures in the composite with  $0 < x < 5$  (Figure

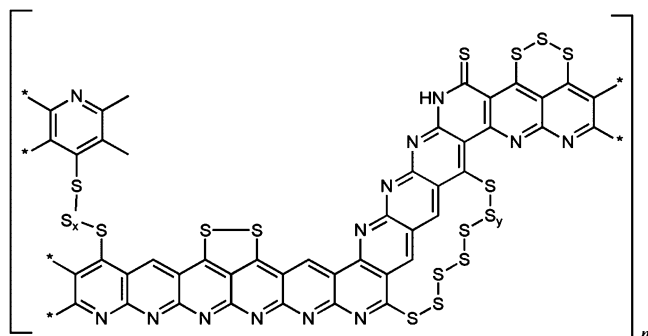


**Figure 3.** Proposed structure of SPAN, containing all relevant functional groups ( $0 < x < 6$ ;  $y = 1, 2$ ).

3). With an XPS-derived thioketone content of  $\leq 20$  at %, a range of  $0 < x \leq 6$  can be calculated. This proposed structure both comprises all observed structural features and explains the observed electrochemistry in terms of capacity, voltage, and cycling behavior.

However, a critical discrepancy is observed in the total amount of sulfur in the charged state. As discussed above, the use of ethers as electrolyte solvent results in fact in larger amounts of soluble poly(sulfide)s that can shuttle to the anode, resulting in a constant loss of active mass in the cathode during cycling. Though both the mass balance and the electrochemical cycling experiments of both ether- and carbonate-based electrolyte solvents strongly suggest the formation of  $\text{S}_8$ , no elemental sulfur can be detected in the charged cathodes by scanning electron microscopy (see Figure S4 in the Supporting Information). This imposes that the sulfur is finely dispersed throughout the SPAN-matrix. The same accounts for  $\text{Li}_2\text{S}$ ,

which can neither be detected by SEM nor by XRD in the discharged state (see Figure S5 in the Supporting Information). Since after each cycle the discharge of carbonate-based electrolyte solvents starts at  $U = 2.1$  V, the direct reduction of  $\text{S}_8$  to  $\text{Li}_2\text{S}$  can in fact be ruled out in these systems. Instead, an activation of  $\text{S}_8$  by the R–S<sup>-</sup> sites of SPAN to form SPAN–S–S<sub>x</sub><sup>-</sup> is proposed. In contrast, ether-based systems, which can dissolve  $\text{S}_8$ , show the direct reduction of  $\text{S}_8$  to  $\text{S}_x^{2-}$  as evidenced by the discharging, which starts at  $U = 2.4$  V (Figure 2b).

Assuming that every sulfur bound to carbon leads to one and all poly(sulfide)s lead to two electrons per sulfur atom, the theoretical capacity of an SPAN device is  $400\text{--}420 \text{ mA h g}_{\text{cathode}}^{-1}$  and thus significantly lower than the actually measured one, which was  $490\text{--}540 \text{ mA h g}_{\text{cathode}}^{-1}$  (first cycle). This corresponds to  $1750\text{--}1800 \text{ mA h g}_{\text{sulfur}}^{-1}$ , which is actually higher than the theoretical capacity of elemental sulfur. Combining the results of sulfur-balance with the ones of the electrochemical measurements, one can calculate an additional capacity of ca.  $100 \text{ mA h g}_{\text{cathode}}^{-1}$  that must stem from an anionic conjugated backbone, as is known for electrically conducting polymers.<sup>24,25</sup> Vice versa, any Li-intercalated graphite as charge carrier can be ruled out since such a system would start discharging at  $0.1 < U < 0.2$  V.<sup>26</sup> Nonetheless, this additional capacity is not observed in the following cycles.

Trying to understand the mechanism of the first discharge and the contribution of the backbone reaction to the total capacity, we established a sulfur balance for the discharge, measuring the amount of covalently bound sulfur for different states of charge (Figure 4). Clearly, the amount of covalently

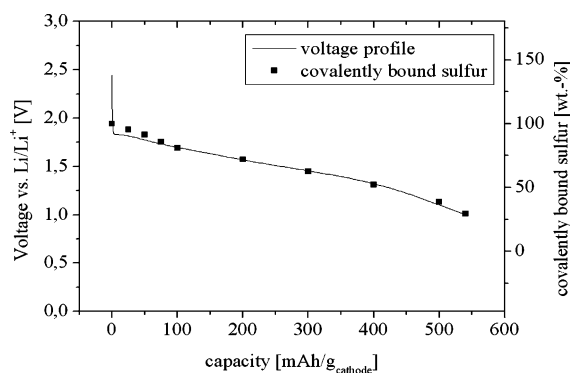


**Figure 4.** Both voltage profile and amount of covalently bound sulfur in the first discharge.

bound sulfur perfectly fits the voltage profile. Thus, at the beginning of discharge, the sulfur chains are broken, resulting in a sulfur content that is somewhat higher due the formation of C–S<sub>x</sub>–SLi instead of free  $\text{Li}_2\text{S}$ . These C–S<sub>x</sub>–SLi moieties are then further reduced, leading to a high loss of covalently bound sulfur up to  $100 \text{ mA h/g}$ . Once  $x$  in C–S<sub>x</sub>–SLi approaches zero, one can envisage a mesomeric rearrangement in the backbone, which results in the formation of Li-thioketones out of lithium thiolates, placing the negative charge at the nitrogen. Ongoing discharge then further reduces the conjugated  $\pi$ -system, which results in a somewhat lower decrease in the amount of covalently bond sulfur between  $100$  and  $400 \text{ mA h/g}_{\text{cathode}}$ . Finally, another increase in the gradient is observed in the last part of discharge ( $Q > 400 \text{ mA h/g}_{\text{cathode}}$ ).

## CONCLUSION

Two different PAN-sulfur composites, i.e., SPAN and ScPAN have been synthesized using a one and a two-step synthetic approach, respectively. In all composites, any remaining elemental sulfur was removed via extraction with toluene. TOF-SIMS, XPS and FT-IR experiments strongly suggest that in all composites the sulfur is exclusively covalently bound to carbon and not to nitrogen. Moreover, N–C–S fragments, most probably resulting from 2-pyridylthiolates as well as  $S_x$  ( $x \geq 2$ ) and thioamide fragments, have been identified by TOF-SIMS. A structure for the composite has been presented that explains for all analytical data as well as for the entire electrochemistry observed. Electrolyte studies showed that the use of ethers, which are capable of dissolving poly(sulfide)s, results in a transport of these poly(sulfide)s away from the cathode and consequently leads to a strong decrease in capacity during cycling. In contrast, the measured capacity does not depend on the nature of the Li-ion conducting salt. Important enough, the polymer backbone, which most probably consists of a conjugated  $\pi$ -system, significantly contributes to the initially measured capacity. Depending on the electrolyte solvents, different activation pathways for intermediary formed  $S_8$  and  $S_x^{2-}$  have been identified. Consequently, an optimum interaction between the electrochemically active backbone, the covalently bound sulfur and the  $S_8$  that forms during recharging are a prerequisite for obtaining both high capacities and good cycling stability.

## ASSOCIATED CONTENT

### Supporting Information

RAMAN spectra of SPAN, cPAN, and ScPAN; XRD spectrum of SPAN; voltage profiles of the first discharge for cells having different sulfur content; SEM pictures of a fresh and a recharged cathode; XRD spectrum of a discharged cathode in a mixture of carbonates. This material is available free of charge via the Internet at <http://pubs.acs.org>.

## AUTHOR INFORMATION

### Corresponding Author

\*E-mail: [michael.buchmeiser@ipoc.uni-stuttgart.de](mailto:michael.buchmeiser@ipoc.uni-stuttgart.de).

## ACKNOWLEDGMENTS

This work was generously supported by the Federal Ministry of Education and Research (BMBF, HE-Lion, 03X4612B).

## REFERENCES

- (1) Ji, X.; Lee, K. T.; Nazar, L. F. *Nature* **2009**, *8*, 500.
- (2) Hassoun, J.; Scrosati, B. *Angew. Chem.* **2010**, *122*, 2421; *Angew. Chem., Int. Ed.* **2010**, *49*, 2371.
- (3) Uemachi, H.; Iwasa, Y.; Mitani, T. *Electrochim. Acta* **2001**, *46*, 2305.
- (4) Tsutsumi, H.; Okada, S.; Oishi, T. *Electrochim. Acta* **1998**, *43*, 427.
- (5) Naoi, K.; Kawase, K.-I.; Inoue, Y. *J. Electrochem. Soc.* **1997**, *144*, L170.
- (6) Huang, L. M.; Wen, T. C.; Yang, C. H. *Mater. Chem. Phys.* **2002**, *77*, 434.
- (7) Jayaprakash, N.; Shen, J.; Moganty, S. S.; Corona, A.; Archer, L. A. *Angew. Chem.* **2011**, *123*, 6026; *Angew. Chem., Int. Ed.* **2011**, *50*, 5904.
- (8) Wang, J.; Yang, J.; Xie, J.; Naixin, X. *Adv. Mater.* **2002**, *14*, 963.
- (9) Huang, X. *Materials* **2009**, *2*, 2369.
- (10) Wang, J.; Yang, J.; Wan, C.; Du, K.; Xie, J.; Xu, N. *Adv. Funct. Mater.* **2003**, *13*, 487.
- (11) Wang, J.; Wang, Y.; He, X.; Ren, J.; Jiang, C.; Wan, C. *J. Power Sources* **2004**, *138*, 271.
- (12) Yu, X.; Xie, J.; Yang, J.; Huang, H.; Wang, K.; Wen, Z. *J. Electroanal. Chem.* **2004**, *573*, 121.
- (13) Yu, X.; Xie, J.; Li, Y.; Huang, H.; Lai, C.; Wang, K. *J. Power Sources* **2005**, *146*, 335.
- (14) Yin, L.; Wang, J.; Yang, J.; Nuli, Y. *J. Mater. Chem.* **2011**, *21*, 6807.
- (15) Morita, K.; Murata, Y.; Ishitani, A.; Murayama, K.; Ono, T.; Nakajima, A. *Pure Appl. Chem.* **1986**, *58*, 455.
- (16) Xue, L. J.; Li, J. X.; Hu, S. Q.; Zhang, M. X.; Zhou, Y. H.; Zhan, C. M. *Electrochem. Commun.* **2003**, *5*, 903.
- (17) Gardella, J. A.; Ferguson, S. A.; Chin, R. L. *Appl. Spectrosc.* **1986**, *40*, 224.
- (18) Braumann, S. K. *J. Polym. Sci., Part A* **1989**, *27*, 3285.
- (19) Moulder, J. F.; Stickle, W. F.; Sobol, P. E.; Bomben, K. D.; ed. Chastain, J.; King, R. C.; Jr., *Handbook of X-ray Photoelectron Spectroscopy*; Physical Electronics Inc.: Eden Prairie, MN, 1995.
- (20) Atzei, D.; de Filippo, D.; Rossi, A. *Spectrochim. Acta* **1995**, *51A*, No. 1, 11.
- (21) Hartung, J.; Weber, G.; Beyer, L.; Szargan, R.; Kreutzmann, J. *Z. Anorg. Allg. Chem.* **1986**, *543*, 186.
- (22) Hesse, M.; Meier, H.; Zeeh, B. *Spektroskopische Methoden in d. org. Chemie*, 7. ü. Auflage; Thieme: Stuttgart, Germany, 2005; Chapter 2.
- (23) Mikhaylik, Y. V.; Akridge, J. R. *Electrochem. Soc.* **2004**, *151*, A1969.
- (24) Heeger, A. *Angew. Chem.* **2001**, *113*, 2660; *Angew. Chem., Int. Ed.* **2001**, *40*, 2591.
- (25) MacDiarmid, A. *Angew. Chem.* **2001**, *113*, 2649; *Angew. Chem., Int. Ed.* **2001**, *40*, 2581.
- (26) Winter, M.; Besenhard, J. O.; Spahr, M. E.; Novak, P. *Adv. Mater.* **1998**, *10*, 725.